Time-Temperature–Transformation (TTT) Diagrams of High T_g Epoxy Systems: Competition Between Cure and Thermal Degradation

L. C. CHAN,* H. N. NAÉ,† and J. K. GILLHAM, *Polymer Materials Program, Department of Chemical Engineering, Princeton University, Princeton, New Jersey 08544*

Synopsis

The cure behavior and thermal degradation of high T_g epoxy systems have been investigated by comparing their isothermal time-temperature-transformation (TTT) diagrams. The formulations were prepared from di- and trifunctional epoxy resins, and their mixtures, with stoichiometric amounts of a tetrafunctional aromatic diamine. The maximum glass transition temperatures ($T_{g\infty}$) were 229°C and > 324°C for the fully cured di- and trifunctional epoxy materials, respectively. Increasing functionality of the reactants decreases the times to gelation and to vitrification, and increases the difference between T_g after prolonged isothermal cure and the temperature of cure. At high temperatures, there is competition between cure and thermal degradation. The latter was characterized by two main processes which involved devitrification (decrease of modulus and T_g) and revitrification (char formation). The experimentally inaccessible $T_{g\infty}$ (352°C) for the trifunctional epoxy material was obtained by extrapolation from the values of $T_{g\infty}$ of the less highly crosslinked systems using a relationship between the glass transition temperature, crosslink density, and chemical structure.

INTRODUCTION

The chemical structures of the reactants in thermosetting systems together with the conditions of cure determine the properties of the cured materials. In order to obtain structure–property relationships, the formulations must be cured above their maximum glass transition temperatures ($T_{g\infty}$) so as to ensure full cure.[1,2] However, for high T_g materials there is competition between cure and thermal degradation at high temperatures.

This article discusses the competition between cure and thermal degradation for high T_g epoxy systems prepared from di- and trifunctional epoxy resins, and their mixtures, cured with stoichiometric amounts of a tetrafunctional aromatic diamine, and the influence of the functionality of the epoxy reactants on cure and the glass transition temperature. The experimentally determined maximum glass transition temperatures ($T_{g\infty}$) were 229°C and > 324°C for the di- and trifunctional epoxy materials, respectively.

A general problem in polymer science is to obtain the values of $T_{g\infty}$ for high T_g polymers in the absence of degradation. The experimentally inaccessable value of $T_{g\infty}$ for the trifunctional epoxy material was obtained by

* Current address: Bell Laboratories, Whippany, NJ 07981.

† Current address: Department of Plastics Research, The Weizmann Institute of Science, Rehovot, Israel 76100.

Journal of Applied Polymer Science, Vol. 29, 3307–3327 (1984)
 CCC 0021-8995/84/113307-21$04.00

an extrapolation method from the less highly crosslinked systems, which involved relating $T_{g\infty}$ to crosslink density and chemical structure.

Isothermal time-temperature-transformation (TTT) diagrams, which display the times to gelation, vitrification, and thermal degradation events, were used for comparing the cure behavior and degradation of the thermosetting systems. A preliminary report has been published.[3] The principal technique was Torsional Braid Analysis (TBA).[1,2,4]

EXPERIMENTAL

Materials

The epoxy systems were formulated from a trifunctional epoxy resin, a difunctional epoxy resin, and a tetrafunctional aromatic diamine. The chemicals were: (I) a triglycidyl ether of tris(hydroxyphenyl)methane (XD7342.00L, Dow Chemical Co., epoxy equivalent weight = 162 g, density = 1.22 g/mL),[5] (II) a diglycidyl ether of bisphenol A (DER 332, Dow Chemical Co., epoxy equivalent weight = 178 g, density = 1.16 g/mL), and (III) 4,4'-diamino diphenyl sulfone (DDS, Aldrich Chemical Co., NH equivalent weight = 62 g). A schematic outline of the reactions is shown in Figure 1. The functionality of the epoxy resins in the formulations was systematically changed by varying the ratio of the equivalents of di- and trifunctional epoxy resins in the formulations. Five stoichiometric formulations (1 equivalent of epoxy with 1 equivalent of amine hydrogen) are included in Table I, which also includes the notation for the systems. Most of the discussion in this paper will focus on the two extreme compositions and the intermediate one (i.e., systems 101, 011, and 112).

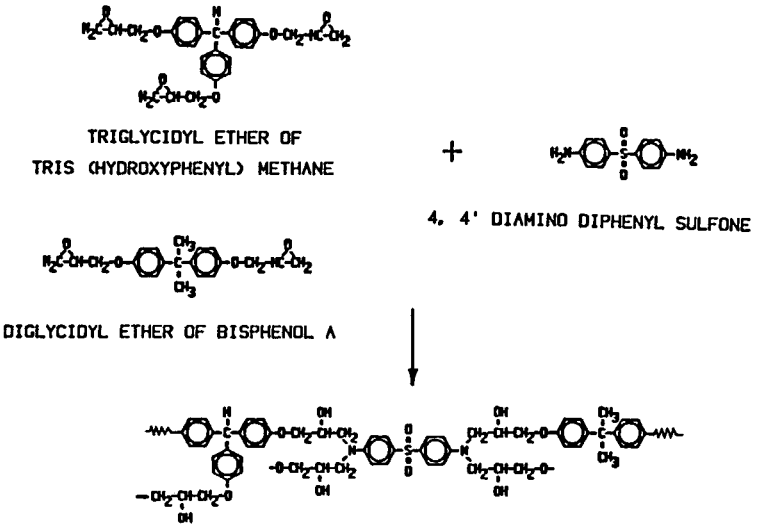

Fig. 1. Schematic outline of the reactions.

TABLE I
Epoxy Systems: Formulations and Notation

System	Equivalents		
	XD 7342 (I)	DER 332 (II)	DDS (III)
101	1	0	1
213	2	1	3
112	1	1	2
123	1	2	3
011	0	1	1

Torsional Braid Analysis

The transformation of a liquid epoxy formulation to a solid polymer during the process of cure and the changes associated with thermal degradation were monitored using a specimen in an automated torsional pendulum instrument [Torsional Braid Analysis (TBA), Plastics Analysis Instruments, Inc.].[4] The specimen was a heat-cleaned (425°C/3 h in air) multifilamented glass braid impregnated with a solution of the reactants in methyl ethyl ketone (volume ratio of the reactants to solvent = 1 to 4). (The different solutions were stored in a refrigerator when not being used.) The pendulum was intermittently set into motion to generate a series of freely damped waves with a natural frequency of 0.05–5 Hz. The change of material behavior of the specimen was monitored as a function of time and/or temperature by computing two dynamic mechanical properties, relative rigidity (modulus) and logarithmic decrement, from the frequency and decay constants that characterize each wave. Isothermal transformations were identified by the times of maxima in the logarithmic decrement. The glass transition temperatures (at ~1 Hz) were identified similarly in the subsequent temperature scans (1.5°C/min). The TBA experiments were performed in helium.

Gel Fraction

The onset of insolubility, which corresponds to the incipient formation of the crosslinked network, was determined from the zero intercept of the extrapolated gel fraction curves. Experimental details follow. The epoxy resin was heated to 130°C in an open beaker and the solid curing agent was added and dissolved (< 5 min) with the aid of mechanical stirring. The solution was degassed at 100°C for 20 min in a preheated vacuum oven at a pressure of about 1 torr and small amounts (1–2 mL) were sealed under helium in ampules, which were then immersed in an oil bath held at a specified temperature. The ampules were removed at selected intervals, quenched in liquid nitrogen, and broken. Gel fractions were measured by weighing the material which remained insoluble in methyl ethyl ketone after 4 h of extraction using a Soxhlet extractor.

Thermogravimetric Analysis

The loss of weight on heating in nitrogen was measured using a thermogravimetric analyzer (TGA, DuPont 950). Temperature scans involved heating uncured samples at a rate of 1.5°C/min. Isothermal experiments were conducted on samples which had been previously cured at 200°C for 24 h in nitrogen.

RESULTS AND DISCUSSION

Cure and Degradation

During the process of cure, an epoxy formulation generally changes sequentially from a liquid, to a rubber, and finally to a glass. Representative isothermal TBA spectra from 80 to 250°C are shown for system 101 in Figure 2. At low temperatures, three events are apparent in the logarithmic decrement (a shoulder and two successive peaks), as is demonstrated by the 125 and 150°C cure spectra. The first peak, which has been designated the liquid-to-rubber transformation (gelation),[1,2] generally corresponds to the onset of insolubility as measured in gel fraction experiments (see below). The shoulder before the gelation peak (which is less apparent at higher temperatures) has been attributed to an isoviscous event which is a consequence of the composite nature of the specimen in the TBA experiment;[1] therefore, it will not be considered further. The second peak, which has been designated the rubber-to-glass transformation (vitrification), occurs

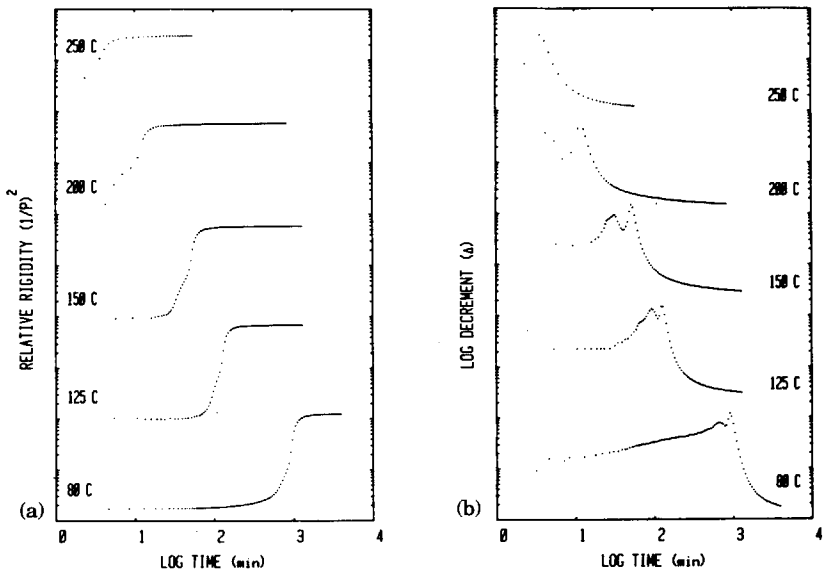

Fig. 2. Representative TBA isothermal spectra for system 101 (80 to 250°C): relative rigidity (a) and logarithmic decrement (b) vs. time.

when the glass transition temperature (T_g) of the material has risen from its initial value (T_{g0}) to the temperature of cure (T_{cure}).[1,2] However the chemical reactions at T_{cure} are essentially quenched only when the resin has become a glass, as is indicated by the leveling off of the relative rigidity (modulus) and the mechanical damping (Δ) beyond the vitrification peak. The glass transition temperature has then risen to a temperature $T_{cure} + \delta T$.[6] The difference (δT) between T_g of the isothermally cured resin and T_{cure} is partly a consequence of the distinction between the quenching of chemical reactions and the operational method for measuring vitrification.[7] (The damping peak for measuring vitrification is located in the middle of the rubber-to-glass transition region as is indicated by the relative rigidity plot, where reactions still occur.) The value of δT is also a function of T_{cure}, time of cure, and the functionality of the reactants (see below).

Representative isothermal TBA spectra for system 101 at higher temperatures (290 to 350°C) are shown in Figure 3. Only the tail end of the vitrification damping peak can be observed (290 and 300°C spectra) due to the high reactivity. However, two major degradation events, each characterized by a broad damping peak, were apparent beyond vitrification. The first event, which is accompanied by a decrease of rigidity, marks the glass-to-rubber transformation (devitrification) and corresponds to the decrease of T_g from above to below the isothermal temperature of cure. The time to this event could be considered as the life time of the material since it marks the limit in time for the material to support a substantial load. The second event, which is accompanied by an increase of rigidity, marks the rubber-to-glass transformation (revitrification) and presumably leads to the for-

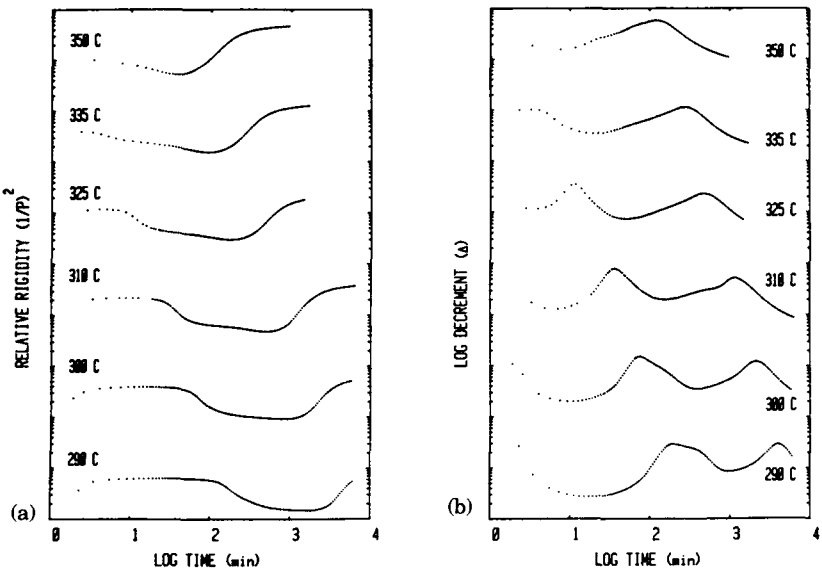

Fig. 3. Representative TBA isothermal spectra for system 101 (290 to 350°C): relative rigidity (a) and logarithmic decrement (b) vs. time.

mation of char. Two additional events are apparent: a shoulder after the devitrification peak (290°C spectrum) and another one before the revitrification peak (310°C spectrum).

Similar cure and degradation behavior were observed in the other systems. Representative isothermal TBA spectra for system 112 are shown in Figure 4. Gelation and vitrification damping peaks are apparent in the 100 and 170°C cure spectra; vitrification and devitrification peaks are apparent in the 270°C spectrum. At temperatures above the maximum glass transition temperature of system 112 ($T_{g\infty}$ = 286°C), the material becomes a gelled rubber and by definition devitrification cannot occur, as is demonstrated by the 325 and 350°C spectra. However, the revitrification process (325 and 350°C spectra) was characterized by a broad damping region which can be resolved into two damping peaks. The two peaks are located at the beginning and at the middle of the rubber-to-glass (revitrification) region, respectively. The latter peak presumably designates the formation of char. An additional event, which involves a decrease of rigidity of the rubbery material, can also be observed as a weak damping shoulder preceding the revitrification region in the 350°C spectrum. For system 011, the revitrification process was characterized by an even broader damping region, which can be resolved into three damping peaks (Fig. 5, 335 and 340°C cure spectra); the last, being located in the middle of the rubber-to-glass (revitrification) region, presumably corresponds to the formation of char. The multiple peaks accompanying revitrification in these two systems (112 and 011) and the occurrence of other events between devitrification and revitrification indicate that degradation is complex.

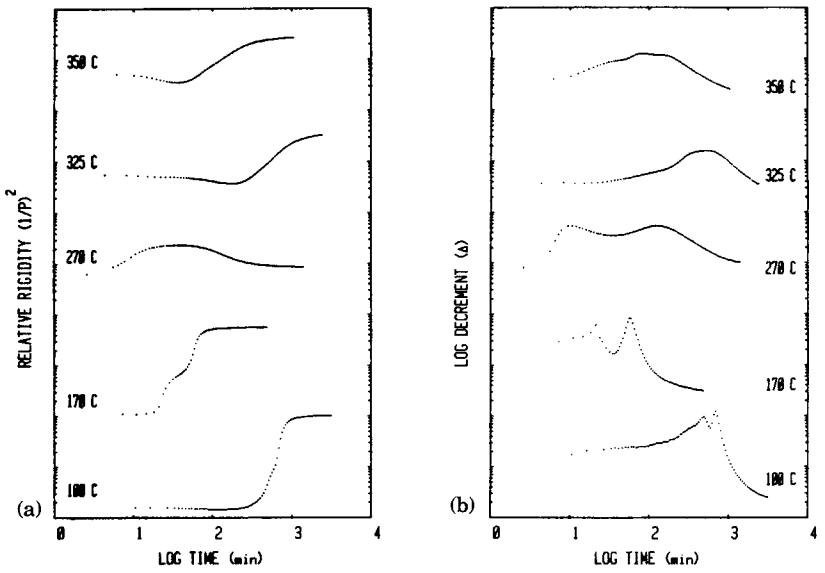

Fig. 4. Representative TBA isothermal spectra for system 112 (100 to 350°C): relative rigidity (a) and logarithmic decrement (b) vs. time.

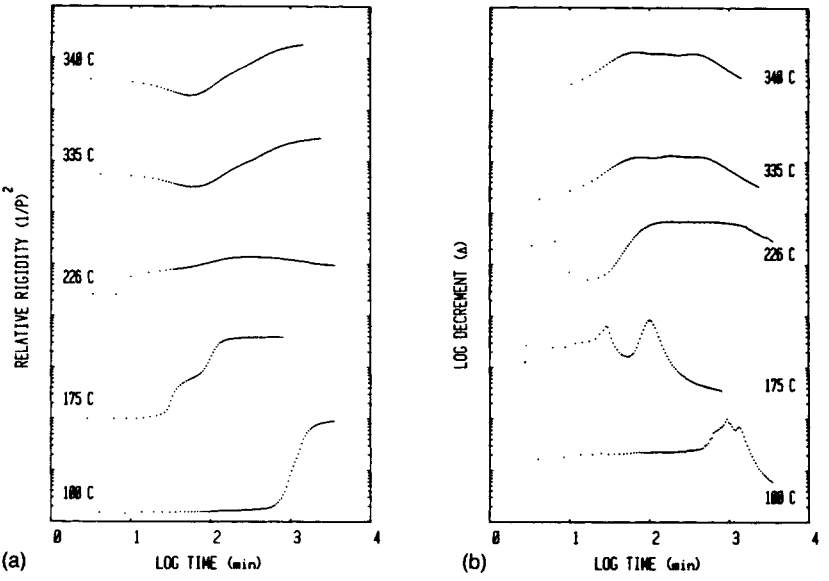

Fig. 5. Representative TBA isothermal spectra for system 011 (100 to 340°C): relative rigidity (a) and logarithmic decrement vs. time.

TGA temperature scans for unreacted formulations of systems 101 and 011 are shown in Figure 6, which shows catastrophic weight loss starting at about 315°C. This event may correspond to the beginning of the devitrification process. The char residue after heating to 470°C was 46% for system 101 and 18% for system 011. Representative isothermal TGA spectra of the precured formulations (200°C/24 h/N_2) of systems 101 and 011 from 225 to 300°C are shown in Figure 7, which shows that degradation is a continuous process, with the weight loss being more rapid in the difunctional epoxy material than in the trifunctional one. In contrast, no weight loss was

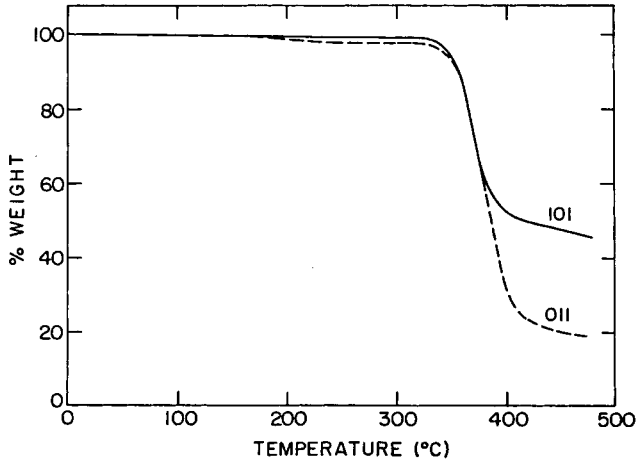

Fig. 6. TGA temperature scans (1.5°C/min) for uncured systems 101 and 011: (——) 101; (- - - -) 011.

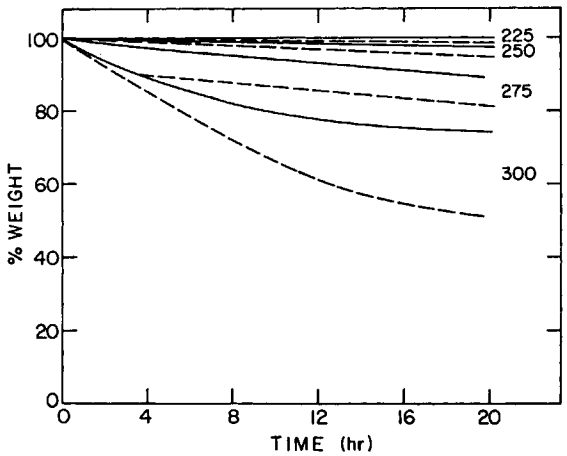

Fig. 7. Representative TGA isothermal spectra for precured systems 101 and 011 (225 to 300°C): (——) 101; (– – –) 011.

detected at 200°C within 28 h for any of the systems. The degradation products of the trifunctional epoxy system were less volatile than those of the difunctional epoxy system because of the higher crosslink density of system 101.

The preliminary report for this research included a "transient" (devitrification/revitrification) degradation event at high temperatures.[3] During the course of further work this was found to be due to the decomposition of organic material (size) on the glass braid, which was removed for subsequent experiments, including those in the present report, by heat-cleaning to 425°C for 3 h in air.

Time–Temperature–Transformation (TTT) Diagram

The times to the different transformations vs. isothermal temperature for the two extreme compositions, 101 and 011, presented in the form of isothermal TTT diagrams, are shown in Figures 8 and 9, respectively. Both diagrams display the times to gelation (liquid-to-rubber transformation), vitrification, devitrification, and revitrification (revitrification for system 011 includes three damping events, the last one of which is designated char formation). Other events (see Cure and Degradation) are not included.

The times which correspond to the onset of insolubility are included in the TTT diagrams (Figs. 8 and 9). In general, the liquid-to-rubber (gelation) curves agree with those obtained from gel fraction experiments, as reported elsewhere.[8,9]

An isothermal TTT diagram is characterized by three principal temperatures:[1,8] T_{g0}, the initial T_g of the system; ${}_{gel}T_g$ the temperature at which the times to gelation and vitrification are the same (or equivalently, the temperature at which the conversions for gelation and vitrification are the same); and $T_{g\infty}$, the maximum glass transition temperature of the fully cured system. The values of the three characteristic temperatures for systems 101, 112, and 011 are included in Table II. Values of T_{g0}, and $T_{g\infty}$

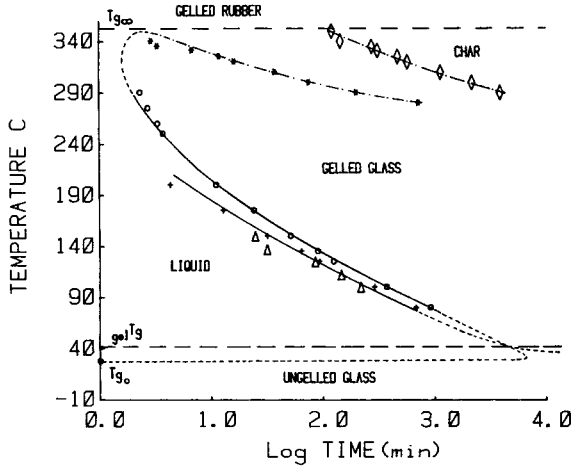

Fig. 8. Isothermal TTT diagram for system 101: (+) liquid-to-rubber (gelation); (o) vitrification (✱) devitrification; (◇) char formation; (△) gel fraction.

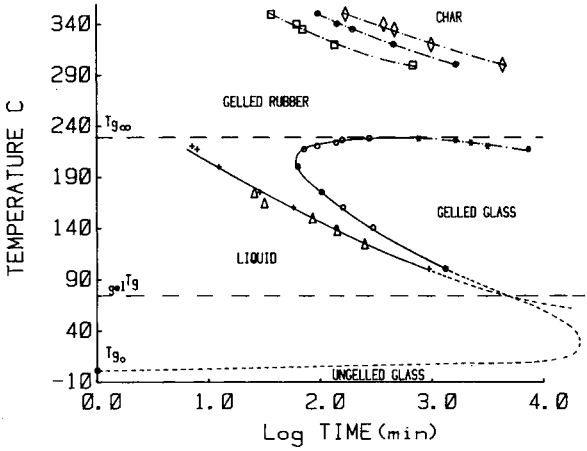

Fig. 9. Isothermal TTT diagram for system 011: (+) liquid-to-rubber (gelation); (o) vitrification; (✱) devitrification; (□) first revitrification event; (⊙) second revitrification event; (◇) third revitrification event (char formation); (△) gel fraction.

TABLE II
TTT Diagrams: Characteristic Parameters

System	T_{g0}[a]	$_{gel}T_g$[a]	$T_{g\infty}$[a]	$_{vit}T_{min}$/time[b]
101	28	~42	352	~315/2
112	13	~72	286	~265/10
011	1	~80	229	~205/60

[a] Characteristic Temperature in °C.
[b] Temperature (°C) at which the time (min) to vitrification is a minimum.

(except for system 101), were obtained from TBA dynamic mechanical spectra of the initial formulations (from 80 to −170°C) and of the fully cured systems (see below), respectively. $T_{g\infty}$ for system 101 is an extrapolated value (see below). Values of ${}_{gel}T_g$ were estimated from the intersection of the gelation and vitrification lines in ln time vs. $1/T\,(K)$ plots (see below). The increasing values of T_{g0} and $T_{g\infty}$ from system 011 to system 101 is a result of the increasing molecular weight of the epoxy resins in the formulations and the increasing crosslink densities in the fully cured materials, respectively. In contrast, the direction of change of ${}_{gel}T_g$ with increasing functionality will be determined by the conversions at gelation, the values of $(T_{g\infty} - T_{g0})$, the values of T_{g0}, and the relationships between T_g (at vitrification) and conversion (Fig. 10).

Each point in the TTT diagram represents a unique state during cure. The liquid region is bounded by gelation (above ${}_{gel}T_g$) and vitrification (below ${}_{gel}T_g$). The gelled rubber region is bounded by gelation and vitrification (above ${}_{gel}T_g$) in the absence of degradation, and also by devitrification and revitrification (char formation) in the presence of degradation. Gelled glass differs from ungelled glass in that the latter will flow on heating (which is the basis of molding technology in the thermosetting industries).

The times to gelation decrease with increasing temperature in an exponential manner as expected from gelation theory.[10] The vitrification curve is generally S-shaped and, in principle, can be computed.[8] The times to vitrification pass through a minimum at a temperature of cure just below $T_{g\infty}$ because of the competing effects of increasing reaction rate constant and increasing extent of conversion at vitrification with increasing temperature. In contrast, the times to vitrification pass through a maximum at a temperature of cure just above T_{g0} because of the competing effects of decreasing viscosity and increasing reactivity with increasing temperature.

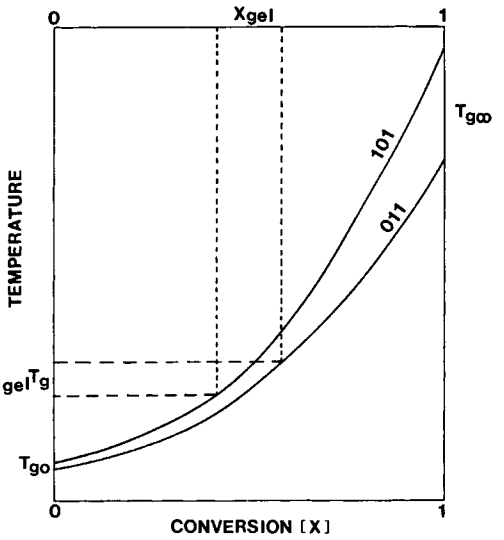

Fig. 10. Schematic: T_g vs. conversion at vitrification for systems 101 and 011. The conversions at gelation are also included. The diagram is useful for demonstrating the effect of increasing functionality on gelation, vitrification, ${}_{gel}T_g$, T_{go}, and $T_{g\infty}$.

According to gelation theory,[10,11] the conversion at gelation decreases with increasing functionality of the reactants. For a system containing a mixture of $A_1, A_2, \ldots, A_i$ moles of monomers with a functionality of $f_1, f_2, \ldots, f_i$, respectively, and $B_1, B_2, \ldots, B_j$ moles of monomers with a functionality of $g_1, g_2, \ldots, g_j$, respectively, in which A's can only react with B's, the conversion at gelation (X_{gel}) is given by:[11,12]

$$X_{gel} = [(f_e - 1)(g_e - 1)]^{-1/2} \quad (1)$$

where

$$f_e = (\Sigma_i f_i^2 A_i)/(\Sigma_i f_i A_i)$$
$$g_e = (\Sigma_j g_j^2 B_j)/(\Sigma_j g_j B_j)$$

The theoretical conversions at gelation for the present systems therefore follow the order: 011 ($X_{gel} = 0.577$) > 112 ($X_{gel} = 0.471$) > 101 ($X_{gel} = 0.408$).

The maximum glass transition temperature increases with increasing crosslink density (see below), which is directly related to the functionality of the reactants, and is responsible for the order of the values of $T_{g\infty}$ for the systems (i.e., 101 > 112 > 011) (Table II). T_g increases with conversion and reaches $T_{g\infty}$ at full conversion:[6,13] at a given cure temperature, the conversion at vitrification should decrease with increasing functionality since T_g at vitrification ($= T_{cure}$) is the further away from its $T_{g\infty}$ the higher the functionality (Fig. 10). Therefore the conversions at vitrification for the system should follow the order: 011 > 112 > 101.

On the basis of the above considerations for the conversions at gelation and vitrification, in terms of time the systems should gel and vitrify in the order 101 < 112 < 011. This is the order found experimentally for isothermal experiments (e.g., compare Figs. 8 and 9). However, it should be noted that the decreasing times to gelation and to vitrification with increasing functionality of the reactants reflects not only the decreasing conversions at gelation and vitrification, but also the increasing rate of reaction due to the lower equivalent weight and higher density of the trifunctional epoxy resin (assuming the reactivity of the glycidyl groups of the di- and trifunctional epoxy resins are the same).

A combined TTT diagram for systems 101, 112, and 011, in which the gelation events have been removed for clarity, is shown in Figure 11. The times to gelation and vitrification decrease with increasing functionality of the epoxy reactants in the systems, as discussed. The minimum times for vitrification immediately below $T_{g\infty}$ also decrease whereas the corresponding temperatures increase with increasing functionality. Estimates for these parameters are included in Table II. The temperature at which the time to vitrification is a minimum is of importance for the economics of molding, in which the cured specimen should be removed only after solidification.

The data for an isothermal TTT diagram can be represented in a ln time vs. $1/T(K)$ plot, from which the apparent activation energies (ΔE) for the transformations can be determined. The ln time vs. $1/T(K)$ plot for system

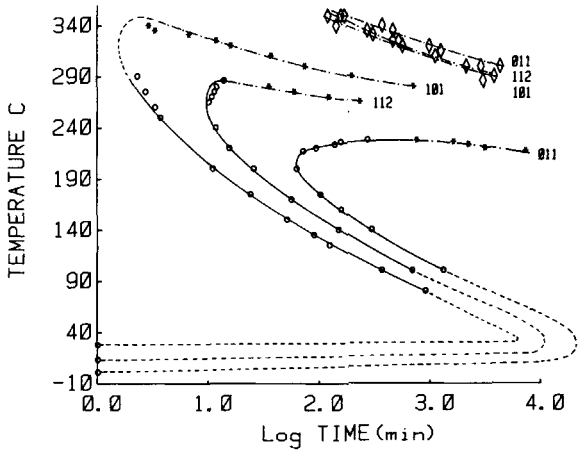

Fig. 11. Combined TTT diagrams for systems 101, 112, and 011: (o) vitrification; (✱) revitrification; (◇) char formation.

101 is presented in Figure 12. The apparent activation energies for gelation, vitrification, devitrification, and char formation for systems 101, 112, and 011 are included in Table III.

Analogous to the isothermal TTT diagram is a continuous-heating-transformation (CHT) diagram which can be constructed from TBA temperature scans of a formulation at different heating rates.[1,2] TTT and CHT diagrams are both relevant to industrial curing processes. Figure 13 shows representative temperature scans from 30 to 325°C at different rates for system 101 which displays gelation, vitrification, and devitrification (T_g) events. The CHT diagram for system 101 in Figure 14 includes the locus of the glass transition temperature of the degraded material after cooling from 325°C at 1.5°C/min. This glass transition temperature is lower than the devitrification temperature because of thermal degradation.

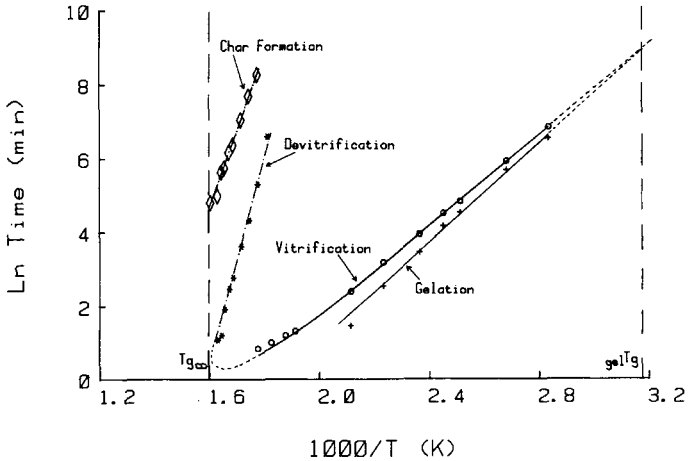

Fig. 12. The ln time vs. 1/T (*K*) for system 101: (+) liquid-to-rubber (gelation); (o) revitrification; (✱) devitrification; (◇) char formation.

TABLE III
Apparent Activation Energies for Isothermal Transformations

System	ΔE^a liquid-to-rubber	$\Delta E^{a,b}$ vitrification	ΔE^a devitrification	ΔE^a char formation
101	13.2	12.1	54.7	42.0
112	14.6	11.6	75.1	36.8
011	15.3	11.3	53.4	42.2

[a] ΔE in kcal/mol, determined from TBA data.

[b] ΔE for vitrification determined from the linear region of the vitrification curve at low temperatures (Fig. 12).

Glass Transition Temperatures

In general, a reacting epoxy system cured isothermally for a prolonged time at temperatures below $T_{g\infty}$ will vitrify before reaching complete conversion to give $T_g < T_{g\infty}$. Upon raising the temperature in a subsequent temperature scan, the vitrified system devitrifies, revitrifies through further reactions, and devitrifies through a glass transition which may reach $T_{g\infty}$ in the absence of degradation. Representative TBA dynamic mechanical spectra for system 101, which were obtained on cooling from T_{cure} to −170°C, heating to 325°C, and cooling to −170°C at a rate of 1.5°C/min, are shown in Figure 15. A broad subzero secondary transition (T_{sec}) at about −40°C and a weak transition below −100°C can be observed. In principle, the T_g

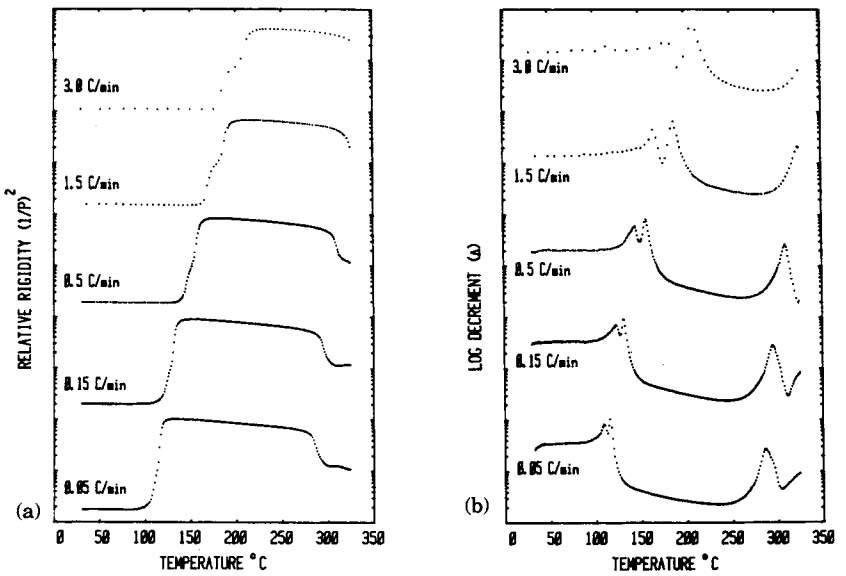

Fig. 13. Representative TBA temperature scans at different heating rates for formulation 101: relative rigidity (a) and logarithmic decrement (b) vs. temperature.

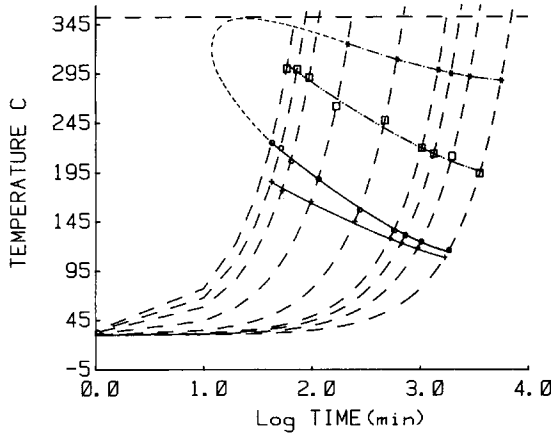

Fig. 14. CHT diagram for system 101: (+) liquid-to-rubber (gelation); (o) vitrification; (*) devitrification; (□) T_g of the degraded material after cooling from 325°C at 1.5°C/min. Temperature Scans: 0.05, 0.1, 0.15, 0.2, 0.5, 1.5, 3.0, 4.0, and 5.0°C/min.

after prolonged isothermal cure at T_{cure} is identified on heating by the first damping maximum above T_{cure}. However, the devitrification and subsequent revitrification processes can occur close together to give merged damping peaks (100 and 150°C spectra) which are sometimes impossible to resolve (150°C spectrum). If the resolution is not possible, the first damping maximum is operationally designated the glass transition temperature after

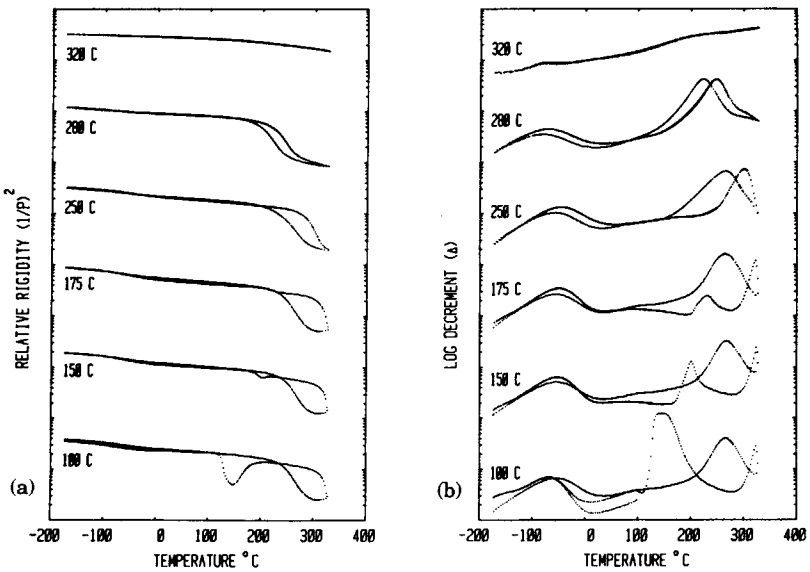

Fig. 15. Representative TBA thermomechanical spectra after prolonged isothermal heating for system 101: relative rigidity (a) and logarithmic decrement (b) vs. temperature.

prolonged isothermal cure at T_{cure} (T_g-as-cured). The damping maximum located at the highest temperature during the temperature scans (up to and down from the upper temperature limit) of the series of materials formed by cure at different isothermal temperatures is operationally designated $T_{g\infty}$ (i.e., the second distinct damping maximum above T_{cure} in the 100°C spectrum on heating to 325°C). The longer the exposure to high temperatures, the greater the degradation and the lower the apparent $T_{g\infty}$ (compare 280 and 150°C spectra). On cooling from the upper limit of temperature (325°C for system 101), the T_g of the degraded material is evident well below $T_{g\infty}$. The dynamic mechanical spectrum of the charred material has only weak features (320°C spectrum).

Representative TBA dynamic mechanical spectra for systems 112 and 011 are shown in Figures 16 and 17, respectively. The upper limits of the temperature scans were 300 and 250°C for systems 112 and 011, respectively. The results paralleled those for system 101. It is noteworthy that the damping peak of T_g-as-cured ($> T_{cure}$) is well resolved from that for revitrification on heating system 112 after cure at 100°C (Fig. 16).

For system 011 (in which the degradation should be negligible on heating to 250°C), it is apparent that the relative rigidity plot of the fully cured material is less than that for the partially cured specimen at, for example, room temperature (RT) (Fig. 17, 100 and 160°C spectra). This implies that the modulus at room temperature (which is below the crossover temperature) for a cured specimen is lower the higher the T_g and extent of conversion (crosslink density). For other high T_g epoxy systems, the decrease in RT

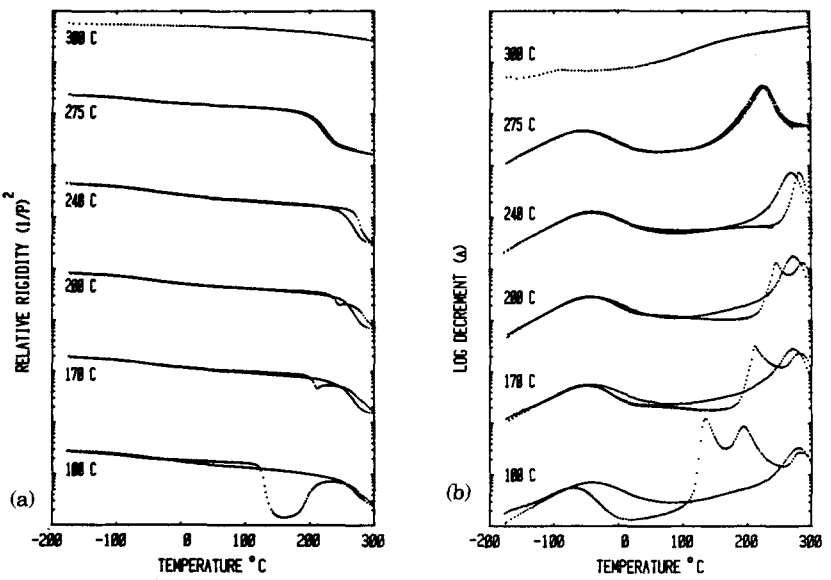

Fig. 16. Representative TBA thermomechanical spectra after prolonged isothermal heating for system 112: relative rigidity (a) and logarithmic decrement (b) vs. temperature.

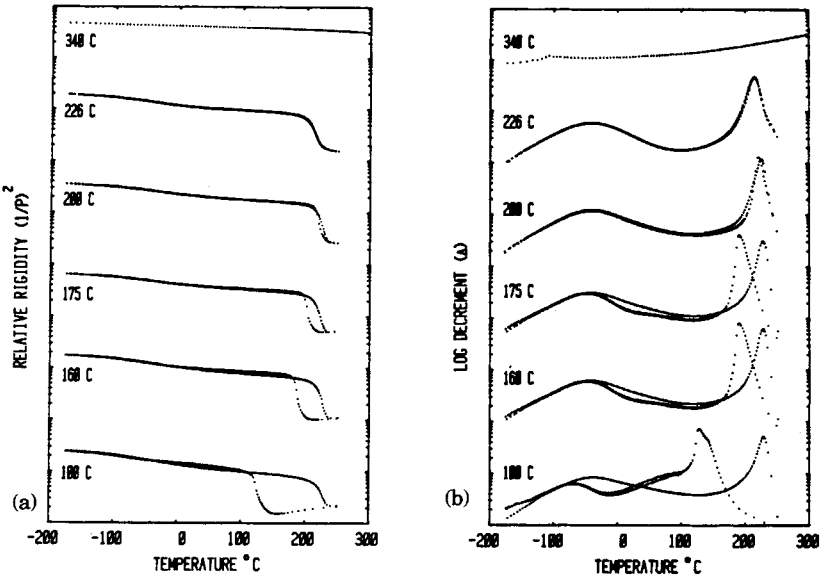

Fig. 17. Representative TBA thermomechanical spectra after prolonged isothermal heating for system 011: relative rigidity (a) and logarithmic decrement (b) vs. temperature.

modulus with increasing extent of cure is paralleled by corresponding decreases in RT density, and increases in RT equilibrium levels of absorbed water.[1,9] A common basis for these interrelated phenomena[9] is the increasing free volume at RT with increasing extent of cure.[14]

The values of T_g and $T_{g\infty}$ vs. temperature of isothermal cure (T_{cure}) for systems 101, 112, and 011 are shown in Figure 18 (data on specimens isothermally cured to devitrification are not included). In the absence of degradation, $T_{g\infty}$ should be independent of the isothermal temperature of cure. In contrast, T_g is dependent on T_{cure}. In general, the difference ($T_g - T_{cure}$) increases with T_{cure} (for $T_{cure} << T_{g\infty}$) and the functionality of the reactants in the system. Increase of ($T_g - T_{cure}$) with increasing functionality is a consequence of the isothermal reactions proceeding further into the glassy state for systems with higher functionality, since the concentration of unreacted groups at vitrification increases with the functionality of the reactants (as discussed). Similarly, part of the increase in ($T_g - T_{cure}$) with increasing functionality can arise from reactions occurring during the temperature scan used to measure T_g; the value of the measured T_g will increase with increasing reactivity.

The increase of the glass transition temperature (ΔT_g) in forming a network is considered to be caused by the introduction of crosslinks ($\Delta_\rho T_g$) and by the change in chemical structure ($\Delta_c T_g$) of the network from that of the monomers.[13,15–17] The latter can also be considered as a copolymer effect.[16,17] The two effects, $\Delta_\rho T_g$ and $\Delta_c T_g$ on ΔT_g have been considered to be independent of each other, being related by the following equation:[13,15–17]

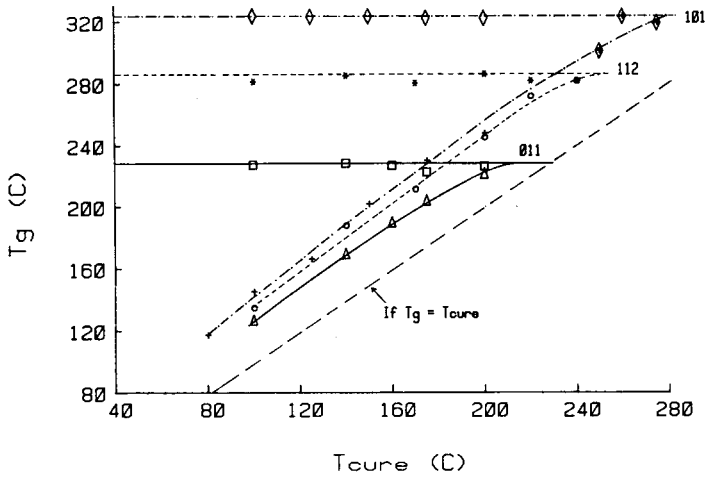

Fig. 18. T_g vs. T_{cure} for systems 101, 112, and 011: (+) T_g-as-cured (101); (◇) apparent $T_{g\infty}$ (101); (o) T_g-as-cured (112); (✱) $T_{g\infty}$ (112); (△) T_g-as-cured (011); (□) $T_{g\infty}$ (011).

$$\Delta T_g = \Delta_\rho T_g + \Delta_c T_g \tag{2}$$

$\Delta_\rho T_g$ is directly related to the degree of crosslinking:[17]

$$\Delta_\rho T_g = K(1/M_c) \tag{3}$$

where M_c = number-average molecular weight between crosslinked junctions (g/mol) and K = a constant (g-°C/mol).

For a fully cured system:

$$\Delta T_g = T_{g\infty} - T_{g0} \tag{4}$$

where $T_{g\infty}$ = maximum transition temperature and T_{g0} = initial glass transition temperature.

Therefore, from eqs. (2), (3), and (4):

$$T_{g\infty} - T_{g0} = K(1/M_c) + \Delta_c T_g \tag{5}$$

For fully cured stoichiometric systems, the number-average molecular weight between crosslinked junctions,

$$M_c = \frac{\text{Total weight of monomers}}{\text{Total number of moles of chain segments in the network}} \tag{6}$$

It is assumed that 1 mol of the trifunctional epoxy resin provides 3 mol of chain segments, 1 mol of the difunctional epoxy resin provides 1 mol of chain segments, and 1 mol of the tetrafunctional aromatic diamine provides 1 mol of chain segments (see Fig. 1). The calculated values of M_c (g/mol)

TABLE IV
Effect of Crosslinking and Chemical Structure on $T_{g\infty}$

System	$T_{g\infty}$	T_{g0}	M_c[a]	$\Delta_p T_g$[b]	$\Delta_c T_g$[c]	Reference
101	352	28	179	220	104	This work
213	309	17	212	186	106	This work
112	286	13	232	170	103	This work
123	267	7	256	154	106	This work
011	229	1	320	123	105	This work
825/DDS[d]	222	0	320	123	99	18
828/DDS[d]	211	11	336	117	83	18
834/DDS[d]	186	20	429	92	74	18
828/MDA[e]	166	−9	319	123	55	18
828/TMAB[f]	167	−2	358	110	59	18
828/PACM-20[g]	166	−19	323	122	63	2, 8

Note. All temperatures are in °C.

[a] Calculated according to text (g/mol)

[b] $\Delta_p T_g = K/M_c$; $K = 0.3933 \times 10^5$.

[c] $\Delta_c T_g = (T_{g\infty} - T_{g0}) - \Delta_p T_g$.

[d] 825, 828, and 834 = Epon 825, Epon 828, and Epon 834, respectively (Shell Chemical Co.). DDS = 4,4'-diamino diphenyl sulfone (Aldrich Chemical Co.).

[e] MDA = methylene dianiline (Aldrich Chemical Co.).

[f] TMAB = trimethylene glycol di-*p*-amino benzoate (Polacure 740M, Polaroid Corp.).

[g] PACM-20 = bis(*p*-amino cyclohexyl)methane (du Pont Chemical Co.).

for systems 101, 213, 112, 123, and 011 were 179, 212, 232, 256, and 320, respectively (Table IV). As expected, the degree of crosslinking ($1/M_c$) increases with increasing functionality of the reactants in the system.

A plot of ($T_{g\infty} - T_{g0}$) vs. $1/M_c$ is shown in Figure 19. A straight line drawn through the values of ($T_{g\infty} - T_{g0}$) for systems 011, 123, 112, and 213 gives a value of K of 0.39×10^5, and a value of $\Delta_c T_g$ of 105°C [eq. (5)]. The value of K is the same as that reported in the literature determined for other crosslinked systems.[17] Extrapolation of these values (Fig. 19) results in $T_{g\infty}$ of the system 101 being 352°C, which is 28°C higher than the directly

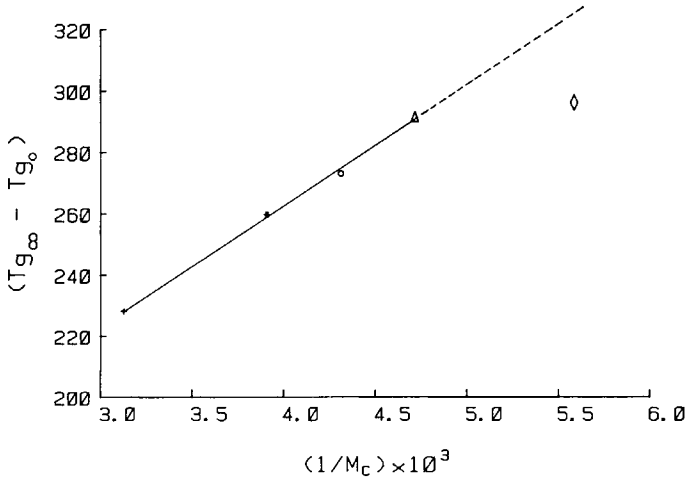

Fig. 19. ($T_{g\infty} - T_{g0}$) vs. $1/M_c$: (+) 011; (✱) 123; (o) 112; (△) 213; (◇) 101.

measured value of $T_{g\infty}$ (= 324°C, ~ 1 Hz). The large difference of the apparent $T_{g\infty}$ and the extrapolated value for system 101 is a consequence of degradation during the temperature scan. The values of $T_{g\infty}$ for other systems might also have been somewhat affected by degradation occurring during the temperature scan, but the effect of degradation on $T_{g\infty}$ should be most acute for system 101 since this system was heated to the highest temperature (325°C) in order to obtain the value of the apparent $T_{g\infty}$.

The values of $\Delta_\rho T_g$ and $\Delta_c T_g$ for systems 101, 213, 112, 123, and 011 are included in Table IV. As expected, the effect of crosslinking ($\Delta_\rho T_g$) increases from system 011 to system 101. $\Delta_c T_g$ is about the same for all the systems, which is a consequence of the similar chemical structures of the reactants [only the relative ratio of $\rangle C(CH_3)_2$ groups in the difunctional epoxy to $\rangle CH$ groups in the trifunctional epoxy differ in the formulations (see Fig. 1)].

Using the same value of K and the calculated values of M_c, and knowing $T_{g\infty}$ and T_{g0}, the values of $\Delta_\rho T_g$ and $\Delta_c T_g$ have been calculated for other diglycidyl ether of bisphenol A (DGEBA)-type epoxy systems cured with tetrafunctional diamines (Table IV). Comparison of the values of $\Delta_\rho T_g$ and $\Delta_c T_g$ shows that the effect of crosslinking is the dominant factor in ΔT_g for all of the systems. The values of $\Delta_\rho T_g$ and $\Delta_c T_g$ for the 825/DDS system are similar to those for system 011 since the reactants in the two systems are essentially the same. The increasing effect of crosslinking from system 834/DDS to system 825/DDS is a consequence of the increasing molecular weight of the difunctional epoxy resins (i.e., 825 < 828 < 834). The difference in $\Delta_c T_g$ between a system containing DDS and a system containing MDA could be attributed to the ability of DDS to form hydrogen bonds which were not taken into consideration in calculating M_c. The system containing TMAB was expected to show a similar trend due to the polarity of the carboxyl groups. This trend is probably overridden by the flexibility of the trimethylene glycol ester segment.

CONCLUSIONS

On cure and in the absence of degradation, increasing functionality of the epoxy reactants in a thermosetting system leads to decreases in the times to gelation and vitrification (which correspond to decreases of the corresponding conversions), and increase in the difference between the glass transition temperature after prolonged isothermal cure and the temperature of cure ($T_{\text{cure}} << T_{g\infty}$), and an increase in the maximum glass transition temperature.

At high temperatures, thermal degradation can interfere with cure. The experimentally inaccessible $T_{g\infty}$ of the trifunctional epoxy material was obtained by an extrapolation method from the less highly crosslinked systems, which involved relating the differences in the glass transition temperatures of the fully cured and uncured systems ($T_{g\infty} - T_{g0}$) to their crosslink densities and chemical structures. This relationship can also be applied to other difunctional epoxy systems cured with tetrafunctional diamines in order to compare the contributions of crosslinking and change of chemical structure to $T_{g\infty}$.

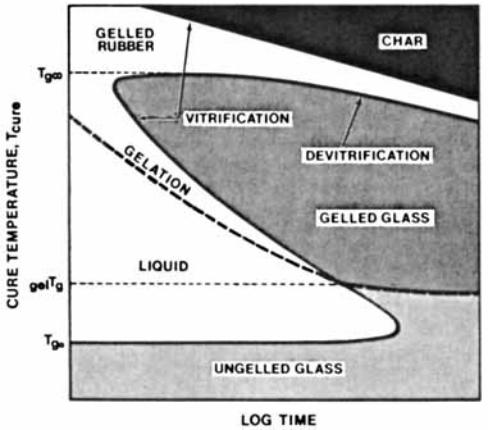

Fig. 20. Schematic isothermal TTT diagram displaying gelation, vitrification, devitrification, and char formation.

Isothermal time-temperature-transformation (TTT) diagrams were used as a basis for understanding and comparing the cure, degradation, and the properties of the systems. This has led to a generalized schematic isothermal TTT diagram (Fig. 20), which displays gelation, vitrification, devitrification (decrease of modulus and T_g), and revitrification (char formation).

Partial financial support has been provided by the Army Research Office.

References

1. J. K. Gillham, in *Developments in Polymer Characterisation-3,* J. V. Dawkins, Ed., Applied Science, London, 1982, pp. 159–227.

2. J. B. Enns and J. K. Gillham, in *Polymer Characterization: Spectroscopic, Chromatographic, and Physical Instrumental Methods,* C. D. Craver, Ed., Advances in Chemistry Series, No. 203, American Chemical Society, Washington, D.C., 1983, pp. 27–63.

3. H. N. Naé and J. K. Gillham, Am. Chem. Soc., Div. Org. Coatings Plast. Chem., Preprint, No. 48, pp. 566–570 (1983).

4. J. B. Enns and J. K. Gillham, in *Computer Applications in Applied Polymer Science,* T. Provder, Ed., ACS Symposium Series, No. 197, American Chemical Society, Washington, D.C., 1982, pp. 329–352.

5. K. L. Hawthorne, Am. Chem. Soc., Div. Org. Coatings Plast. Chem., Preprint, No. 46, p. 493 (1982).

6. L. C. Chan, J. K. Gillham, A. J. Kinloch, and S. J. Shaw, in *Rubber-Modified Thermoset Resins,* C. K. Riew and J. K. Gillham, Eds., Advances in Chemistry Series No. 209, American Chemical Society, Washington, D.C., 1984, chap. 15.

7. *High-Performance, Low-Energy-Curing Resins,* National Materials Advisory Board, National Research Council, Publication NMAB-412, National Academy Press, Washington, D.C., 1984.

8. J. B. Enns and J. K. Gillham, *J. Appl. Polym. Sci.,* **28**, 2567 (1983).

9. J. B. Enns and J. K. Gillham, *J. Appl. Polym. Sci.,* **28**, 2831 (1983).

10. P. J. Flory, in *Principles of Polymer Chemistry,* Cornell Univ. Press, Ithaca, New York, 1953.

11. W. H. Stockmayer, *J. Polym. Sci.,* **9**, 69 (1952); **11**, 424 (1953).

12. C. W. Macosko and D. R. Miller, *Macromolecules,* **9**, 199 (1976).

13. K. Horie, H. Iura, M. Sawada, I. Mita, and H. Kambe, *J. Polym. Sci., A1,* **8**, 1357 (1970).

14. A. Shimazaki, *J. Polym. Sci., Part C,* **23**, 555 (1968).
15. T. G. Fox and S. Loshaek, *J. Polym. Sci.,* **15**, 371 (1955).
16. S. Loshaek, *J. Polym. Sci.,* **15**, 391 (1955).
17. L. E. Nielsen, *J. Macromol. Sci., Revs.,* **C3**(1), 69 (1969).
18. J. B. Enns, Ph.D. Thesis, Princeton University, Princeton, 1982.

Received December 6, 1982
Accepted February 22, 1983
Revised manuscript received May 31, 1984